

# NUMERICAL SIMULATION AND OPTIMAL SHAPE FOR VISCOUS FLOW BY A FICTITIOUS DOMAIN METHOD

ROLAND GLOWINSKI\* AND TSORNG-WHAY PAN

*Department of Mathematics, University of Houston, Houston, TX 77204, U.S.A.*

ANTHONY J. KEARSLEY

*Department of Computational and Applied Mathematics, Rice University, Houston, TX 77251-1892, U.S.A.*

JACQUES PERIAUX

*Dassault Aviation, 92214 Saint-Cloud, France*

## SUMMARY

In this article we discuss the fictitious domain solution of the Navier–Stokes equations modelling unsteady incompressible viscous flow. The method is based on a Lagrange multiplier treatment of the boundary conditions to be satisfied and is particularly well suited to the treatment of no-slip boundary conditions. This approach allows the use of structured meshes and fast specialized solvers for problems on complicated geometries. Another interesting feature of the fictitious domain approach is that it allows the solution of optimal shape problems without regriding. The resulting methodology is applied to the solution of flow problems including external incompressible viscous flow modelled by the Navier–Stokes equations and then to an optimal shape problem for Stokes and Navier–Stokes flow.

KEY WORDS: fictitious domain methods; Lagrange multipliers; Navier–Stokes equations; optimal shape problems

## 1. INTRODUCTION

Fictitious domain methods for partial differential equations are showing interesting possibilities for solving complicated problems motivated by applications from Science and Engineering (see, for example, References 1 and 2 for some impressive illustrations of the above statement). The main reason for the popularity of fictitious domain methods (sometimes called *domain embedding methods*; cf. Reference 3) is that they allow the use of fairly structured meshes on a simple shape auxiliary domain containing the actual one. This allows the use of fast solvers.

In this article, which follows References 4–6, we consider the fictitious domain solution of the Navier–Stokes equations modelling the unsteady flow of incompressible Newtonian viscous fluids and apply the resulting methodology to the solution of optimal shape problems for Stokes and Navier–Stokes flows.

Since the methods discussed here are a generalization of the Lagrange multiplier-based techniques described in Reference 4, we shall first discuss the fictitious domain solution of linear Dirichlet problems, then show how it generalizes to the Navier–Stokes equations. Finally, we

---

\* Also at Université P. et M. Curie, Paris and CERFACS, Toulouse, France

combine these ideas with non-linear programming algorithms to solve optimal shape problems for Stokes and Navier–Stokes flows.

The methods discussed here go far beyond the related work in Reference 7 where only the steady Stokes problem was considered (in the particular case where the boundary of the actual domain is compatible with the finite element mesh used in the auxiliary domain). The methods described in the following sections do not require a strong coupling between the actual boundary discretization and the grid used in the auxiliary domain. It also relies on the splitting methods described in, e.g., References 8–12; with these methods one can decouple the numerical treatments of the incompressibility and of the advection, and take the advantage of this fact to use the embedding approach in the (linear) incompressibility step only, the advection being treated in the larger domain without concern—in some sense—for the actual boundary.

The content of this article is as follows: In Section 2 we consider the Dirichlet problem; then in Section 3 we consider the simulation of external incompressible viscous flow modelled by Navier–Stokes equations with Neumann downstream boundary condition. In Section 4 we address the fictitious domain solution of optimal shape problems for Stokes and Navier–Stokes flows. Finally, in Section 5 we conclude the paper with some observations and comments on future work.

## 2. A FICTITIOUS DOMAIN METHOD FOR THE DIRICHLET PROBLEM

### 2.1. A model problem

Let  $\omega$  be a bounded domain of  $\mathbb{R}^d$  ( $d \geq 1$ ) and let us denote by  $\gamma$  its boundary  $\partial\omega$ ; we suppose that  $\gamma$  is Lipschitz-continuous. We consider the following Dirichlet problem:

$$\begin{aligned} &\text{Given } f \in H^{-1}(\omega), \quad g \in H^{1/2}(\gamma), \quad \text{find a function } u \text{ such that} \\ &\alpha u - \nu \Delta u = f \text{ in } \omega \\ &u = g \text{ on } \gamma \end{aligned} \tag{1}$$

where  $\alpha \geq 0$  and  $\nu > 0$ . Problem (1) has a unique solution  $u$  in  $H^1(\omega)$ .

### 2.2. A fictitious domain formulation

For simplicity, we shall assume from now on that  $f \in L^2(\omega)$ . A fictitious domain method was already proposed for problem (1) in Reference 4. This method is as follows: let us consider a ‘box’  $\Omega$  which is a domain in  $\mathbb{R}^d$  such that  $\omega \subset\subset \Omega$  (see Figure 1) and denote by  $\Gamma$  the boundary of  $\Omega$ .

Problem (1) is equivalent to the following problem:

$$\begin{aligned} &\text{Find } \{\tilde{u}, \lambda\} \in V \times L^2(\gamma) \text{ such that} \\ &\int_{\Omega} (\alpha \tilde{u} v + \nu \nabla \tilde{u} \cdot \nabla v) \, dx = \int_{\Omega} \tilde{f} v \, dx + \int_{\gamma} \lambda v \, d\gamma, \quad \forall v \in V \\ &\int_{\gamma} \mu (\tilde{u} - g) \, d\gamma = 0, \quad \forall \mu \in L^2(\gamma) \end{aligned} \tag{2}$$

where  $\tilde{f} \in L^2(\Omega)$  and satisfies  $\tilde{f}|_{\omega} = f$  and  $V$  is a well chosen closed subspace of  $H^1(\Omega)$ . Natural choices for  $V$  are  $H^1(\Omega)$ ,  $H_0^1(\Omega)$ , and

$$H_P^1(\Omega) = \{v \mid v \in H^1(\Omega), v \text{ is periodic at } \Gamma\}$$

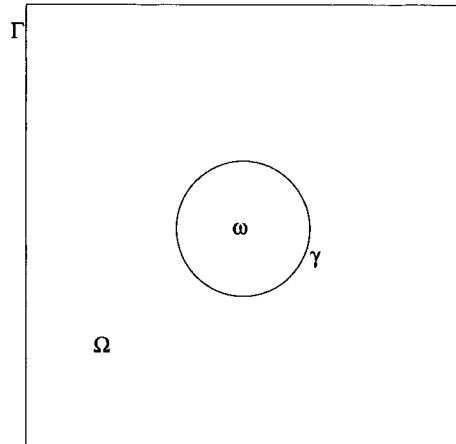


Figure 1

In (2) let  $v|_{\omega} \in H_0^1(\omega)$  and  $v = 0$  in  $\Omega \setminus \bar{\omega}$ , then  $\tilde{u}$  satisfies

$$\int_{\Omega} (\alpha \tilde{u} v + v \nabla \tilde{u} \cdot \nabla v) \, d\mathbf{x} = \int_{\omega} \tilde{f} v \, d\mathbf{x}, \quad \forall v \in H_0^1(\omega)$$

Also we have  $\tilde{u} = g$  on  $\gamma$ . Thus  $\tilde{u}|_{\omega}$  is the solution of problem (1). The reciprocal property is also quite easy to prove; it is essentially based on Green's theorem. More precisely, in (2), we have that the multiplier  $\lambda$  is equal to  $v[\partial \tilde{u} / \partial \mathbf{n}]|_{\gamma}$  (i.e.,  $v$  times the jump of the normal derivative of  $\tilde{u}$  at  $\gamma$ ).

*Remark 2.1.* By using penalization technique, we can obtain another fictitious domain formulation for the Dirichlet problem (1), namely

Find  $\tilde{u}_{\varepsilon} \in V$  such that

$$\begin{aligned} \int_{\Omega} (\alpha \tilde{u}_{\varepsilon} v + v \nabla \tilde{u}_{\varepsilon} \cdot \nabla v) \, d\mathbf{x} + \frac{1}{\varepsilon} \int_{\gamma} \tilde{u}_{\varepsilon} v \, d\gamma &= \int_{\Omega} \tilde{f} v \, d\mathbf{x} + \frac{1}{\varepsilon} \int_{\gamma} g v \, d\gamma, \quad \forall v \in V \end{aligned} \tag{3}$$

where, in (3),  $\varepsilon > 0$ . It can be easily shown (see, e.g., Appendix 1 in Reference 8) that

$$\lim_{\varepsilon \rightarrow 0} \|\tilde{u}_{\varepsilon} - u\|_{H^1(\omega)} = 0$$

where  $u$  is the solution of (1).

### 2.3. Conjugate gradient solution and preconditioning

Applying the general conjugate gradient methodology to problem (2), we obtain

$$\lambda^0 \in L^2(\gamma) \text{ given} \tag{4}$$

solve

$$\text{Find } u^0 \in V \text{ such that} \quad (5)$$

$$\int_{\Omega} (\alpha u^0 v + v \nabla u^0 \cdot \nabla v) \, d\mathbf{x} = \int_{\Omega} \tilde{f} v \, d\mathbf{x} + \int_{\gamma} \lambda^0 v \, d\gamma, \quad \forall v \in V$$

and then

$$\text{Find } g^0 \in L^2(\gamma) \text{ such that} \quad (6)$$

$$\int_{\gamma} g^0 \mu \, d\gamma = \int_{\gamma} (u^0 - g) \mu \, d\gamma, \quad \forall \mu \in L^2(\gamma)$$

and set

$$w^0 = g^0. \quad (7)$$

For  $n \geq 0$ , assuming that  $\lambda^n, g^n, w^n$  are known, compute  $\lambda^{n+1}, g^{n+1}, w^{n+1}$ , as follows:  
solve

$$\text{Find } \bar{u}^n \in V \text{ such that} \quad (8)$$

$$\int_{\Omega} (\alpha \bar{u}^n v + v \nabla \bar{u}^n \cdot \nabla v) \, d\mathbf{x} = \int_{\gamma} w^n v \, d\gamma, \quad \forall v \in V$$

compute

$$\rho_n = \int_{\gamma} |g^n|^2 \, d\gamma / \int_{\gamma} \bar{u}^n w^n \, d\gamma \quad (9)$$

set

$$\lambda^{n+1} = \lambda^n - \rho_n w^n \quad (10)$$

$$u^{n+1} = u^n - \rho_n \bar{u}^n \quad (11)$$

and then solve

$$\text{Find } g^{n+1} \in L^2(\gamma) \text{ such that} \quad (12)$$

$$\int_{\gamma} g^{n+1} \mu \, d\gamma = \int_{\gamma} g^n \mu \, d\gamma - \rho_n \int_{\gamma} \bar{u}^n \mu \, d\gamma, \quad \forall \mu \in L^2(\gamma).$$

If  $\|g^{n+1}\|_{L^2(\gamma)} / \|g^0\|_{L^2(\gamma)} \leq \varepsilon$ , take  $\lambda = \lambda^{n+1}$ ,  $\tilde{u} = u^{n+1}$ ; if not compute

$$\gamma_n = \|g^{n+1}\|_{L^2(\gamma)}^2 / \|g^n\|_{L^2(\gamma)}^2 \quad (13)$$

and set

$$w^{n+1} = g^{n+1} + \gamma_n w^n \quad (14)$$

Do  $n = n + 1$  and go to (8)

*Remark 2.2.* For the cases where  $\omega \subset \mathbb{R}^2$  with a smooth boundary  $\gamma$ , we have obtained a quasi-optimal preconditioner for the conjugate gradient algorithm (4)–(14) by Fourier Analysis (see Reference 4).

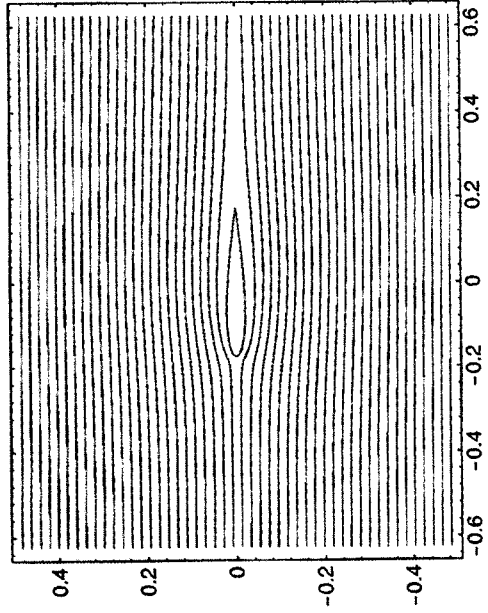
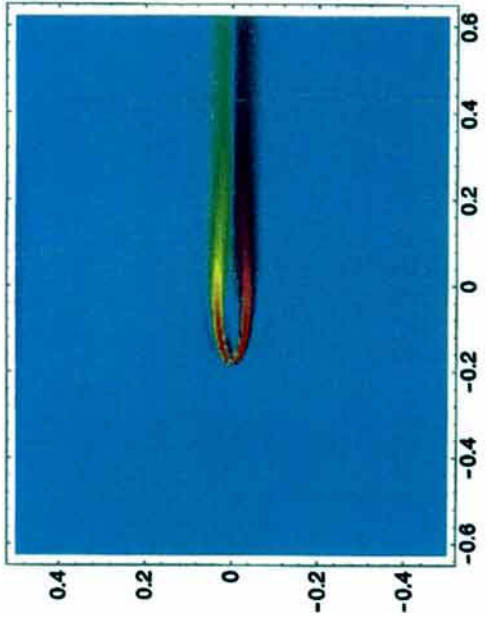


Plate 1. Vorticity density (top) and streamlines (bottom) for the flow passing around NACA0012 with zero degree angle of attack. Flow direction is from the left to the right, the Reynolds number is 1000, dimensionless time is 1-8

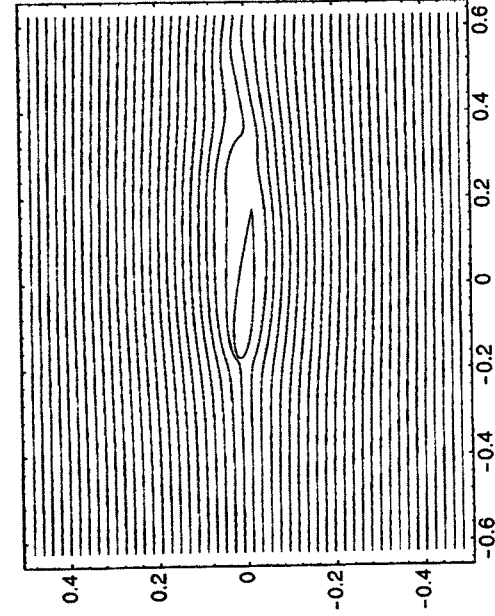
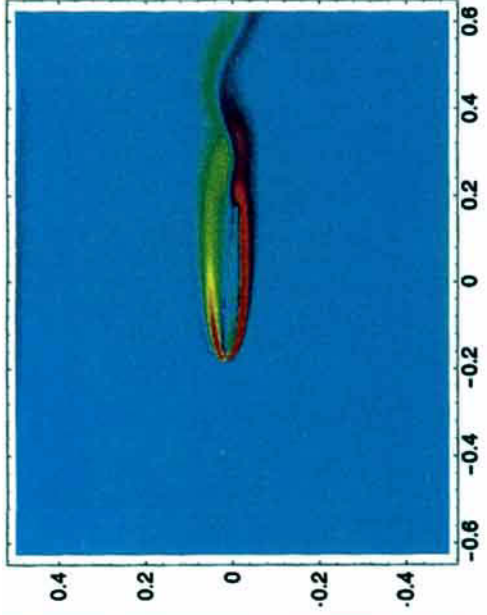


Plate 2. Vorticity density (top) and streamlines (bottom) for the flow passing around NACA0012 with 5 degrees angle of attack. Flow direction is from the left to the right, the Reynolds number is 1000, dimensionless time is 1-34

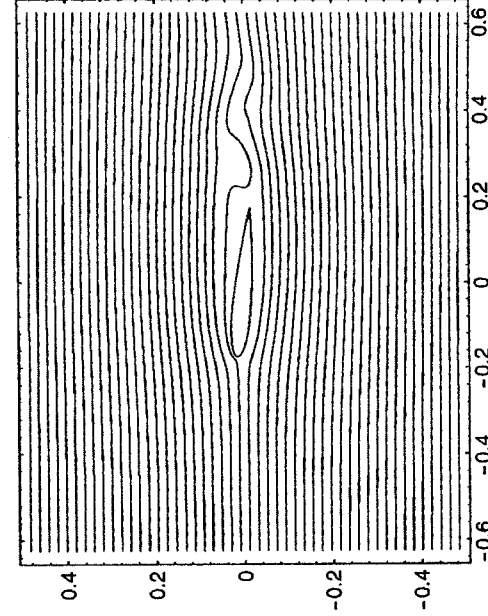
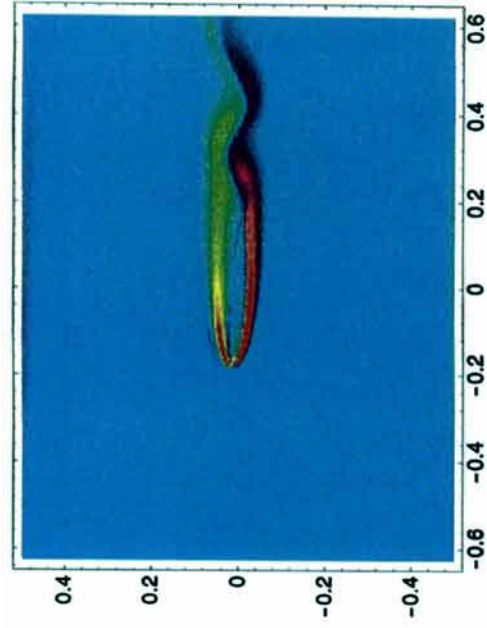


Plate 3. Vorticity density (top) and streamlines (bottom) for the flow passing around NACA0012 with 5 degrees angle of attack. Flow direction is from the left to the right, the Reynolds number is 1000, dimensionless time is 1-525

#### 2.4. Finite element implementation

The finite element implementation of the above conjugate gradient algorithms (4)–(14) is a straightforward modification. For the space  $V$  occurring in problem (2), we have taken  $V = H^1_p(\Omega)$ . For the finite-dimensional subspaces,  $V_h \subset V$  and  $\Lambda_h \subset L^2(\gamma)$ , we took

$$V_h = \{v_h \mid v_h \in V \cap C^0(\bar{\Omega}), v_h|_T \in P_1, \forall T \in \mathcal{T}_h\}, \quad (15)$$

where  $\mathcal{T}_h$  is a triangulation of  $\Omega$  (see, e.g., Figure 2) and  $P_1$  is the space of the polynomials in 2 variables of degree  $\leq 1$  and

$$\Lambda_h = \{\mu_h \mid \mu_h = \text{constant on the segment joining 2 consecutive mesh points on } \gamma\}. \quad (16)$$

The mesh on  $\gamma$  can be uniform as visualized in Figure 2 (where we have shown the mesh points on  $\gamma$ ), but this is not a necessity. The numerical results which have been obtained clearly suggest that both  $L^2(\omega)$ -error and  $L^\infty(\omega)$ -error are *second-order accurate*. Moreover, in the absence of a preconditioner the number of conjugate gradient iterations increases as  $h^{-1/2}$ . This is what we expect from a theoretical point of view; with preconditioning the number of iterations is ‘almost’ constant, as shown in Reference 4. The above method has been applied to the solution of *three-dimensional* problems, still showing second-order accuracy.<sup>5</sup>

*Remark 2.3.* Compared to previous domain embedding methods our method does not require the adjustment of the mesh to the geometry of  $\omega$  and  $\gamma$ . Indeed the spaces  $V_h$  and  $\Lambda_h$  are largely independent and it is strongly advised to define  $\Lambda_h$  from the intrinsic geometrical properties of  $\gamma$ . This is particularly well suited to these situations where  $\omega$  is subjected to rigid body motions. Of course the fact that  $V_h$  is defined from a structured triangulation of  $\Omega$  provides substantial simplification to the numerical implementation on parallel machines.<sup>13</sup>

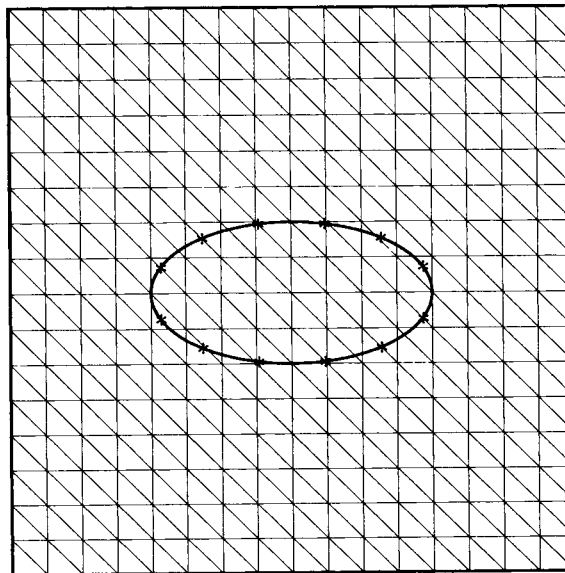


Figure 2. Mesh for  $V_h$  with  $h = 1/16$  and mesh on  $\gamma$  ( $\Omega = (0, 1)^2$ )

### 3. EXTERNAL INCOMPRESSIBLE VISCOUS FLOW

In Reference 5, we have considered external incompressible viscous flow modelled by the Navier–Stokes equations with Dirichlet downstream boundary conditions. In this section we would like to consider the problem with Neumann boundary conditions downstream since they are less reflecting than the Dirichlet boundary conditions.

#### 3.1. The Navier–Stokes equations

Using the notation in Figure 3, we consider the following problem:

$$\frac{\partial \mathbf{u}}{\partial t} - \nu \nabla \mathbf{u} + (\mathbf{u} \cdot \nabla) \mathbf{u} + \nabla p = \mathbf{f} \quad \text{in } \Omega \setminus \bar{\omega} \quad (17)$$

$$\nabla \cdot \mathbf{u} = 0 \quad \text{in } \Omega \setminus \bar{\omega} \quad (18)$$

$$\mathbf{u}(\mathbf{x}, 0) = \mathbf{u}_0(\mathbf{x}), \quad \mathbf{x} \in \Omega \setminus \bar{\omega}, \quad (\text{with } \nabla \cdot \mathbf{u}_0 = 0) \quad (19)$$

$$\mathbf{u} = \mathbf{g}_0 \quad \text{on } \Gamma_0, \quad \nu \frac{\partial \mathbf{u}}{\partial \mathbf{n}} - \mathbf{n}p = \mathbf{g}_1 \quad \text{on } \Gamma_1 \quad (20)$$

$$\mathbf{u} = \mathbf{g}_2 \quad \text{on } \gamma \quad (21)$$

In (17)–(21),  $\Omega$  and  $\omega$  are bounded domains in  $\mathbb{R}^d$  ( $d \geq 2$ ) (see Figure 3),  $\Gamma$  (resp.,  $\gamma$ ) is the boundary of  $\Omega$  (resp.,  $\omega$ ) with  $\Gamma = \Gamma_0 \cup \Gamma_1$ ,  $\Gamma_0 \cap \Gamma_1 = \emptyset$ . And  $\int_{\Gamma_1} d\Gamma > 0$ ,  $\mathbf{n}$  is the outer normal unit vector at  $\Gamma_1$ ,  $\mathbf{u} = \{u_i\}_{i=1}^d$  is the flow velocity,  $p$  is the pressure,  $\mathbf{f}$  is a density of external forces,  $\nu$  ( $> 0$ ) is a viscosity parameter, and

$$(\mathbf{v} \cdot \nabla) \mathbf{w} = \left\{ \sum_{j=1}^{j=d} v_j \frac{\partial w_i}{\partial x_j} \right\}_{i=1}^{i=d}$$

To obtain the equivalent fictitious domain formulation for the Navier–Stokes equations, we embed  $\Omega \setminus \bar{\omega}$  in  $\Omega$  and define

$$\mathbf{V}_{\mathbf{g}_0} = \{ \mathbf{v} \mid \mathbf{v} \in (\mathbf{H}^1(\Omega))^d, \mathbf{v} = \mathbf{g}_0 \text{ on } \Gamma_0 \} \quad (22)$$

$$\mathbf{V}_0 = \{ \mathbf{v} \mid \mathbf{v} \in (\mathbf{H}^1(\Omega))^d, \mathbf{v} = \mathbf{0} \text{ on } \Gamma_0 \} \quad (23)$$

$$\Lambda = (\mathbf{L}^2(\gamma))^d \quad (24)$$

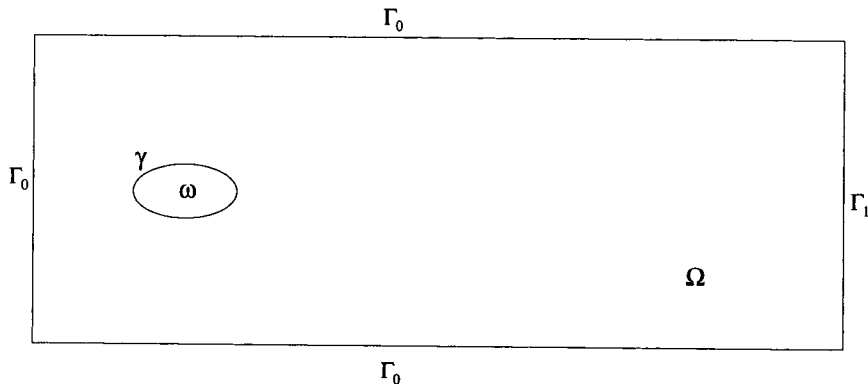


Figure 3

We observe that if  $\mathbf{U}_0$  is an extension of  $\mathbf{u}_0$  with  $\nabla \cdot \mathbf{U}_0 = 0$  in  $\Omega$ , and if  $\tilde{\mathbf{f}}$  is an extension of  $\mathbf{f}$ , we have equivalence between (17)–(21) and the following problem:

For  $t > 0$ , find  $\mathbf{U}(t) \in \mathbf{V}_{\mathbf{g}_0}$ ,  $P(t) \in \mathbf{L}^2(\Omega)$ ,  $\lambda(t) \in \Lambda$  such that

$$\begin{aligned} & \int_{\Omega} \frac{\partial \mathbf{U}}{\partial t} \cdot \mathbf{v} \, d\mathbf{x} + \nu \int_{\Omega} \nabla \mathbf{U} \cdot \nabla \mathbf{v} \, d\mathbf{x} + \int_{\Omega} (\mathbf{U} \cdot \nabla) \mathbf{U} \cdot \mathbf{v} \, d\mathbf{x} - \int_{\Omega} P \nabla \cdot \mathbf{v} \, d\mathbf{x} \\ &= \int_{\Omega} \tilde{\mathbf{f}} \cdot \mathbf{v} \, d\mathbf{x} + \int_{\Gamma_1} \mathbf{g}_1 \cdot \mathbf{v} \, d\Gamma + \int_{\gamma} \lambda \cdot \mathbf{v} \, d\gamma, \quad \forall \mathbf{v} \in \mathbf{V}_0, \text{ a.e. } t > 0 \end{aligned} \tag{25}$$

$$\nabla \cdot \mathbf{U}(t) = 0 \quad \text{in } \Omega \tag{26}$$

$$\mathbf{U}(\mathbf{x}, 0) = \mathbf{U}_0(\mathbf{x}), \quad \mathbf{x} \in \Omega, \quad (\text{with } \nabla \cdot \mathbf{U}_0 = 0) \tag{27}$$

$$\mathbf{U}(t) = \mathbf{g}_2(t) \quad \text{on } \gamma \tag{28}$$

in the sense that  $\mathbf{U}|_{\Omega \setminus \bar{\omega}} = \mathbf{u}$ ,  $P|_{\Omega \setminus \bar{\omega}} = p$ .

Concerning the multiplier  $\lambda$ , its interpretation is very simple since it is equal to the jump of

$$\nu \frac{\partial \mathbf{U}}{\partial \mathbf{n}} - \mathbf{n}P$$

at  $\gamma$ . A closely related approach (limited to the steady Stokes problem) is discussed in Reference 7. We observe that the effect of the actual geometry is concentrated on  $\int_{\gamma} \lambda \cdot \mathbf{v} \, d\gamma$  in the right-hand side of (25), and on (28).

### 3.2. Time discretization by operator splitting

To solve (25)–(28), we shall consider a time discretization by an *operator splitting method*, like the ones discussed in e.g., References 8–12. With these methods we are able to *decouple* the non-linearity and the incompressibility in the Navier–Stokes/fictitious domain problems (25)–(28). In the following, we consider the time discretization of (25)–(28) by the  $\theta$ -scheme (cf. Reference 12) with  $\Delta t > 0$  a time discretization step. Let

$$\mathbf{V}_{\mathbf{g}_0^s} = \{ \mathbf{v} \mid \mathbf{v} \in (\mathbf{H}^1(\Omega))^d, \mathbf{v} = \mathbf{g}_0(s\Delta t) \text{ on } \Gamma_0 \} \tag{29}$$

We obtain the following scheme:

$$\mathbf{U}^0 = \mathbf{U}_0 \text{ is given} \tag{30}$$

for  $n \geq 0$ , knowing  $\mathbf{U}^n$ , find  $\mathbf{U}^{n+\theta} \in \mathbf{V}_{\mathbf{g}_0^{n+\theta}}$ ,  $P^{n+\theta} \in \mathbf{L}^2(\Omega)$ ,  $\lambda^{n+\theta} \in \Lambda$  such that

$$\begin{aligned} & \int_{\Omega} \frac{\mathbf{U}^{n+\theta} - \mathbf{U}^n}{\theta \Delta t} \cdot \mathbf{v} \, d\mathbf{x} + \alpha \nu \int_{\Omega} \nabla \mathbf{U}^{n+\theta} \cdot \nabla \mathbf{v} \, d\mathbf{x} \\ & - \int_{\Omega} P^{n+\theta} \nabla \cdot \mathbf{v} \, d\mathbf{x} - \int_{\gamma} \lambda^{n+\theta} \cdot \mathbf{v} \, d\gamma \\ &= \int_{\Omega} \tilde{\mathbf{f}}^{n+\theta} \cdot \mathbf{v} \, d\mathbf{x} - \int_{\Omega} (\mathbf{U}^n \cdot \nabla) \mathbf{U}^n \cdot \mathbf{v} \, d\mathbf{x} - \beta \nu \int_{\Omega} \nabla \mathbf{U}^n \cdot \nabla \mathbf{v} \, d\mathbf{x} \\ & + \int_{\Gamma_1} \mathbf{g}_1^{n+\theta} \cdot \mathbf{v} \, d\Gamma, \quad \forall \mathbf{v} \in \mathbf{V}_0 \end{aligned} \tag{31}$$



$$\nabla \cdot \mathbf{U}^{n+\theta} = 0 \quad \text{in } \Omega \quad (32)$$

$$\mathbf{U}^{n+\theta} = \mathbf{g}_2^{n+\theta} \quad \text{on } \gamma \quad (33)$$

next find  $\mathbf{U}^{n+1-\theta} \in \mathbf{V}_{\mathbf{g}_0^{n+1-\theta}}$  such that

$$\begin{aligned} & \int_{\Omega} \frac{\mathbf{U}^{n+1-\theta} - \mathbf{U}^{n+\theta}}{(1-2\theta)\Delta t} \cdot \mathbf{v} \, d\mathbf{x} + \beta \nu \int_{\Omega} \nabla \mathbf{U}^{n+1-\theta} \cdot \nabla \mathbf{v} \, d\mathbf{x} \\ & + \int_{\Omega} (\mathbf{U}^{n+1-\theta} \cdot \nabla) \mathbf{U}^{n+1-\theta} \cdot \mathbf{v} \, d\mathbf{x} \\ & = \int_{\Omega} \tilde{\mathbf{f}}^{n+1-\theta} \cdot \mathbf{v} \, d\mathbf{x} + \int_{\gamma} \lambda^{n+\theta} \cdot \mathbf{v} \, d\gamma \quad (34) \\ & - \int_{\Omega} P^{n+\theta} \nabla \cdot \mathbf{v} \, d\mathbf{x} - \alpha \nu \int_{\Omega} \nabla \mathbf{U}^{n+\theta} \cdot \nabla \mathbf{v} \, d\mathbf{x} \\ & + \int_{\Gamma_1} \mathbf{g}_1^{n+1-\theta} \cdot \mathbf{v} \, d\Gamma, \quad \forall \mathbf{v} \in \mathbf{V}_0 \end{aligned}$$

finally, find  $\mathbf{U}^{n+1} \in \mathbf{V}_{\mathbf{g}_0^{n+1}}$ ,  $P^{n+1} \in L^2(\Omega)$ ,  $\lambda^{n+1} \in \Lambda$  such that

$$\begin{aligned} & \int_{\Omega} \frac{\mathbf{U}^{n+1} - \mathbf{U}^{n+1-\theta}}{\theta \Delta t} \cdot \mathbf{v} \, d\mathbf{x} + \alpha \nu \int_{\Omega} \nabla \mathbf{U}^{n+1} \cdot \nabla \mathbf{v} \, d\mathbf{x} \\ & - \int_{\Omega} P^{n+1} \nabla \cdot \mathbf{v} \, d\mathbf{x} - \int_{\gamma} \lambda^{n+1} \cdot \mathbf{v} \, d\gamma \quad (35) \\ & = \int_{\Omega} \tilde{\mathbf{f}}^{n+1} \cdot \mathbf{v} \, d\mathbf{x} - \int_{\Omega} (\mathbf{U}^{n+1-\theta} \cdot \nabla) \mathbf{U}^{n+1-\theta} \cdot \mathbf{v} \, d\mathbf{x} \\ & - \beta \nu \int_{\Omega} \nabla \mathbf{U}^{n+1-\theta} \cdot \nabla \mathbf{v} \, d\mathbf{x} + \int_{\Gamma_1} \mathbf{g}_1^{n+1} \cdot \mathbf{v} \, d\Gamma, \quad \forall \mathbf{v} \in \mathbf{V}_0 \end{aligned}$$

$$\nabla \cdot \mathbf{U}^{n+1} = 0 \quad \text{in } \Omega \quad (36)$$

$$\mathbf{U}^{n+1} = \mathbf{g}_2^{n+1} \quad \text{on } \gamma \quad (37)$$

where  $\alpha + \beta = 1$ ,  $0 < \alpha, \beta < 1$  and  $0 < \theta < 1/2$ . With the choice of  $\theta = 1 - 1/\sqrt{2}$ ,  $\alpha = 2 - \sqrt{2}$  and  $\beta = \sqrt{2} - 1$ , the time discretization seems to be unconditionally stable (see Reference 12).

In Section 3.3 the conjugate gradient solution of the *Stokes/fictitious domain problems* (31)–(33) and (35)–(37) shall be discussed. Concerning problem (34) it is worth noticing that we have been taking advantage of the time discretization by operator splitting to treat the advection in the larger domain  $\Omega$  without concern—in some sense—for the constraint  $\mathbf{u} = \mathbf{g}$  at  $\gamma$ . Problem (34) can be solved by least-squares methods<sup>12</sup> and is also well suited to solution methods based on higher-order upwinding on regular meshes, or on the backward method of characteristics (see, e.g., Reference 14).

3.3. Iterative solution to the Stokes/fictitious domain problem

Problems (31)–(33) and (35)–(37) are particular cases of the following Stokes/fictitious domain problem:

Find  $\mathbf{U} \in \mathbf{V}_{g_0}$ ,  $P \in L^2(\Omega)$ ,  $\lambda \in \Lambda$  such that

$$\alpha \int_{\Omega} \mathbf{U} \cdot \mathbf{v} \, d\mathbf{x} + \nu \int_{\Omega} \nabla \mathbf{U} \cdot \nabla \mathbf{v} \, d\mathbf{x} - \int_{\Omega} P \nabla \cdot \mathbf{v} \, d\mathbf{x} \tag{38}$$

$$= \int_{\Omega} \mathbf{f} \cdot \mathbf{v} \, d\mathbf{x} + \int_{\gamma} \lambda \cdot \mathbf{v} \, d\gamma + \int_{\Gamma_1} \mathbf{g}_1 \cdot \mathbf{v} \, d\Gamma, \quad \forall \mathbf{v} \in \mathbf{V}_0$$

$$\nabla \cdot \mathbf{U} = 0 \quad \text{in } \Omega \tag{39}$$

$$\mathbf{U} = \mathbf{g}_2 \quad \text{on } \gamma \tag{40}$$

where, in (38),  $\alpha (> 0)$  is the reciprocal of a partial time step. In this saddle-point system,  $P$  (resp.,  $\lambda$ ) appear to be a Lagrange multiplier associated with (39) (resp., (40)).

We can solve the above saddle-point system (38)–(40) by a conjugate gradient algorithm called a one-shot method driven by the pressure  $P$  and the multiplier  $\lambda$ , simultaneously.

Let us consider a bilinear form  $b(\cdot, \cdot)$ , symmetric and strongly elliptic over  $\Lambda$ . The following algorithm is a one-shot method driven by the multipliers  $P$  and  $\lambda$ :

$$\{P^0, \lambda^0\} \in L^2(\Omega) \times \Lambda \text{ given} \tag{41}$$

solve the following Dirichlet problem:

Find  $\mathbf{U}^0 \in \mathbf{V}_{g_0}$ , such that

$$\begin{aligned} \alpha \int_{\Omega} \mathbf{U}^0 \cdot \mathbf{v} \, d\mathbf{x} + \nu \int_{\Omega} \nabla \mathbf{U}^0 \cdot \nabla \mathbf{v} \, d\mathbf{x} &= \int_{\Omega} \mathbf{f} \cdot \mathbf{v} \, d\mathbf{x} \\ + \int_{\gamma} \lambda^0 \cdot \mathbf{v} \, d\gamma + \int_{\Omega} P^0 \nabla \cdot \mathbf{v} \, d\mathbf{x} + \int_{\Gamma_1} \mathbf{g}_1 \cdot \mathbf{v} \, d\Gamma, \quad \forall \mathbf{v} \in \mathbf{V}_0 \end{aligned} \tag{42}$$

set

$$\mathbf{r}_1^0 = \nabla \cdot \mathbf{U}^0, \quad \mathbf{r}_2^0 = (\mathbf{U}^0 - \mathbf{g}_2)|_{\gamma} \tag{43}$$

and define  $\mathbf{g}^0 = \{g_1^0, \mathbf{g}_2^0\}$  as follows

$$g_1^0 = \alpha \phi^0 + \nu r_1^0 \tag{44}$$

with  $\phi^0$  the solution of

$$\begin{aligned} -\Delta \phi^0 &= r_1^0 \quad \text{in } \Omega \\ \frac{\partial \phi^0}{\partial \mathbf{n}} &= 0 \quad \text{on } \Gamma_0; \quad \phi^0 = 0 \quad \text{on } \Gamma_1 \end{aligned} \tag{45}$$

$$\mathbf{g}_2^0 \in \Lambda \tag{46}$$

$$b(\mathbf{g}_2^0, \mu) = \int_{\gamma} \mathbf{r}_2^0 \cdot \mu \, d\gamma, \quad \forall \mu \in \Lambda$$

We take

$$\mathbf{w}^0 = \{w_1^0, \mathbf{w}_2^0\} = \{g_1^0, \mathbf{g}_2^0\} \tag{47}$$

Then for  $n \geq 0$ , assuming that  $\{P^n, \lambda^n\}, \mathbf{U}^n, r_1^n, \mathbf{r}_2^n, \mathbf{w}^n, \mathbf{g}^n$  are known, compute  $\{P^{n+1}, \lambda^{n+1}\}, \mathbf{U}^{n+1}, r_1^{n+1}, \mathbf{r}_2^{n+1}, \mathbf{w}^{n+1}, \mathbf{g}^{n+1}$  as follows:

solve

Find  $\bar{\mathbf{U}}^n \in \mathbf{V}_0$ , such that

$$\begin{aligned} & \alpha \int_{\Omega} \bar{\mathbf{U}}^n \cdot \mathbf{v} \, d\mathbf{x} + \nu \int_{\Omega} \nabla \bar{\mathbf{U}}^n \cdot \nabla \mathbf{v} \, d\mathbf{x} \\ & = \int_{\gamma} \mathbf{w}_2^n \cdot \mathbf{v} \, d\gamma + \int_{\Omega} w_1^n \nabla \cdot \mathbf{v} \, d\mathbf{x}, \quad \forall \mathbf{v} \in \mathbf{V}_0 \end{aligned} \quad (48)$$

set

$$\bar{r}_1^n = \nabla \cdot \bar{\mathbf{U}}^n, \quad \bar{r}_2^n = \bar{\mathbf{U}}^n|_{\gamma} \quad (49)$$

and define  $\bar{\mathbf{g}}^n = \{\bar{g}_1^n, \bar{\mathbf{g}}_2^n\}$  as follows:

$$\bar{g}_1^n = \alpha \bar{\phi}^n + \nu \bar{r}_1^n \quad (50)$$

with  $\bar{\phi}^n$  the solution of

$$\begin{aligned} -\Delta \bar{\phi}^n &= \bar{r}_1^n \quad \text{in } \Omega \\ \frac{\partial \bar{\phi}^n}{\partial \mathbf{n}} &= 0 \quad \text{on } \Gamma_0; \quad \bar{\phi}^n = 0 \quad \text{on } \Gamma_1 \end{aligned} \quad (51)$$

$$\bar{\mathbf{g}}_2^n \in \Lambda \quad (52)$$

$$b(\bar{\mathbf{g}}_2^n, \mu) = \int_{\gamma} \bar{r}_2^n \cdot \mu \, d\gamma, \quad \forall \mu \in \Lambda$$

We compute then

$$\rho_n = \frac{\int_{\Omega} r_1^n g_1^n \, d\mathbf{x} + \int_{\gamma} \mathbf{r}_2^n \cdot \mathbf{g}_2^n \, d\gamma}{\int_{\Omega} \bar{r}_1^n w_1^n \, d\mathbf{x} + \int_{\gamma} \bar{r}_2^n \cdot \mathbf{w}_2^n \, d\gamma} \quad (53)$$

and set

$$P^{n+1} = P^n - \rho_n w_1^n \quad (54)$$

$$\lambda^{n+1} = \lambda^n - \rho_n \mathbf{w}_2^n \quad (55)$$

$$\mathbf{U}^{n+1} = \mathbf{U}^n - \rho_n \bar{\mathbf{U}}^n \quad (56)$$

$$r_1^{n+1} = r_1^n - \rho_n \bar{r}_1^n \quad (57)$$

$$\mathbf{r}_2^{n+1} = \mathbf{r}_2^n - \rho_n \bar{\mathbf{r}}_2^n \quad (58)$$

$$g_1^{n+1} = g_1^n - \rho_n \bar{g}_1^n \quad (59)$$

$$\mathbf{g}_2^{n+1} = \mathbf{g}_2^n - \rho_n \bar{\mathbf{g}}_2^n \quad (60)$$

If

$$\frac{\int_{\Omega} r_1^{n+1} g_1^{n+1} \, d\mathbf{x} + \int_{\gamma} \mathbf{r}_2^{n+1} \cdot \mathbf{g}_2^{n+1} \, d\gamma}{\int_{\Omega} r_1^0 g_1^0 \, d\mathbf{x} + \int_{\gamma} \mathbf{r}_2^0 \cdot \mathbf{g}_2^0 \, d\gamma} \leq \varepsilon$$

take  $P = P^{n+1}$ ,  $\mathbf{U} = \mathbf{U}^{n+1}$  and  $\lambda = \lambda^{n+1}$ . If not, compute

$$\gamma_n = \frac{\int_{\Omega} r_1^{n+1} g_1^{n+1} \, d\mathbf{x} + \int_{\gamma} \mathbf{r}_2^{n+1} \cdot \mathbf{g}_2^{n+1} \, d\gamma}{\int_{\Omega} r_1^n g_1^n \, d\mathbf{x} + \int_{\gamma} \mathbf{r}_2^n \cdot \mathbf{g}_2^n \, d\gamma} \tag{61}$$

and set

$$\mathbf{w}^{n+1} = \mathbf{g}^n + \gamma_n \mathbf{w}^n \tag{62}$$

Do  $n = n + 1$  and go back to (48).

We may choose

$$b(\lambda, \mu) = \int_{\gamma} \lambda \cdot \mu \, d\gamma, \quad \forall \lambda, \mu \in \Lambda$$

If we do so, the one shot method described here combines the conjugate gradient method for the Dirichlet problem discussed in Section 2.3 with the quasi-optimal preconditioned conjugate gradient method for solving the Stokes problem described in Reference 12.

### 3.4. Numerical experiments

We consider the test problems where  $\omega$  is a NACA0012 airfoil with zero degree or 5 degrees angle of attack centered at  $(0, 0)$  and  $\Omega$  is  $(-0.625, 0.625) \times (-0.5, 0.5)$  (see Figure 4) where the chord length of NACA0012 is 0.35. The boundary conditions are defined as follows:

$$\mathbf{u} = \begin{cases} (1 - e^{-c\alpha}) \begin{pmatrix} 1 \\ 0 \end{pmatrix} & \text{on } \Gamma_0 \\ \mathbf{0} & \text{on } \gamma \end{cases} \tag{63}$$

$$v \frac{\partial \mathbf{u}}{\partial \mathbf{n}} - \mathbf{n}p = \mathbf{0} \quad \text{on } \Gamma_1 \tag{64}$$

where  $c$  is a positive constant.

As a finite dimensional subspace of  $\mathbf{V}$ , we choose

$$\mathbf{V}_h = \{ \mathbf{v}_h \mid \mathbf{v}_h \in H_{0h}^1 \times H_{0h}^1 \}$$

where

$$H_{0h}^1 = \{ \phi_h \mid \phi_h \in C^0(\bar{\Omega}), \phi_h|_T \in P_1, \forall T \in \mathcal{T}_h, \phi_h = 0 \text{ on } \Gamma_0 \}$$

$\mathcal{T}_h$  is a triangulation of  $\Omega$  (see, e.g., Figure 5),  $P_1$  being the space of the polynomials in  $x_1, x_2$  of degree  $\leq 1$ . A traditional way of approximating the pressure is to take it in the space

$$H_{2h}^1 = \{ \phi_h \mid \phi_h \in C^0(\bar{\Omega}), \phi_h|_T \in P_1, \forall T \in \mathcal{T}_{2h} \}$$

where  $\mathcal{T}_{2h}$  is a triangulation twice coarser than  $\mathcal{T}_h$ . Concerning the space  $\Lambda_h$  approximating  $\Lambda$ , we define it by

$$\Lambda_h = \{ \mu_h \mid \mu_h \in (L^\infty(\partial\omega))^2, \mu_h \text{ is constant on the segment joining 2 consecutive mesh points on } \partial\omega \}$$

A particular choice for the mesh points on  $\gamma$  is visualized on Figure 5. A choice of the mesh points on  $\gamma$  depends on the distribution of the curvature of  $\gamma$ . Around the leading edge, we have to put more mesh points there. Also at the trailing edge, we have to choose mesh points carefully. With

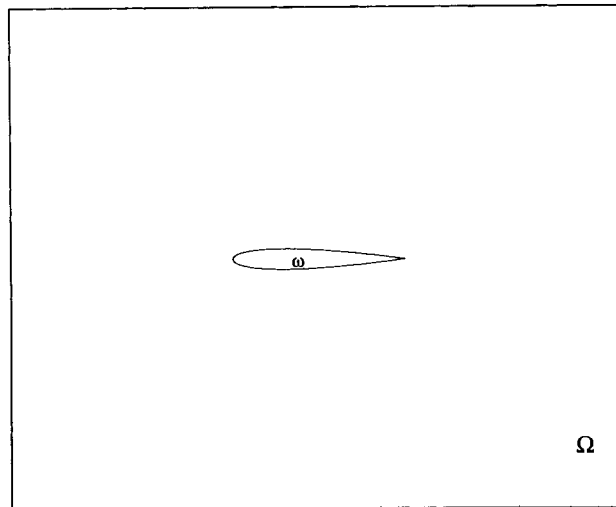
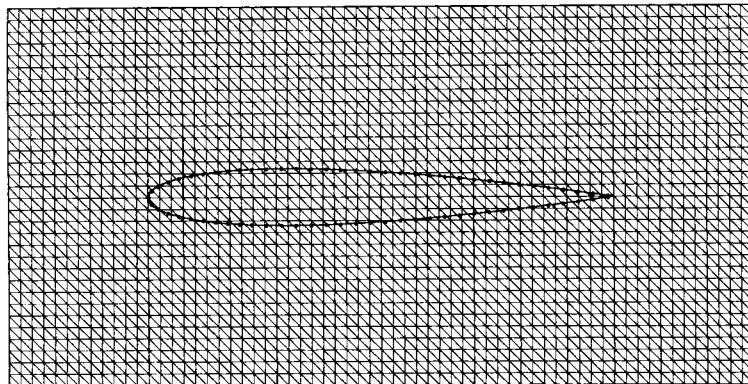


Figure 4

Figure 5. Mesh of  $\gamma$  where 'o' are the mesh points on  $\gamma$  and part of the triangulation of  $\Omega$  with meshsize  $h = 1/128$ 

a bad choice of mesh points on  $\gamma$  (e.g., an uniform mesh on  $\gamma$ ), the Dirichlet boundary condition can not be matched very well for the case where the ratio of  $\alpha$  and  $\nu$  in (38) is of the order  $10^8$ .

The numerical results have been obtained for Reynolds number 1000 (taking the chord of airfoil as *characteristic length*) with meshsizes  $h_v = 1/256$  for velocity and  $h_p = 1/128$  for pressure, time step  $\Delta t = 0.0025$  and  $c$  in (63) is 20. In Plate 1, angle of attack is zero degree and the vorticity and stream function distributions are almost symmetric with respect to the  $x$  direction for the part of the flow behind the airfoil. For the case where angle of attack is 5 degrees, the *Kàrmàn vortex shedding* occurs (see Plates 2 and 3). The local enlargement of streamlines distribution around NACA0012 of Plates 2 and 3 are shown in Figures 6 and 7.

#### 4. SHAPE OPTIMIZATION OF THE BOUNDARY

Shape optimization problems governed by partial differential equations have always been problems of interest leading to many interesting applications (see for example References 15 and

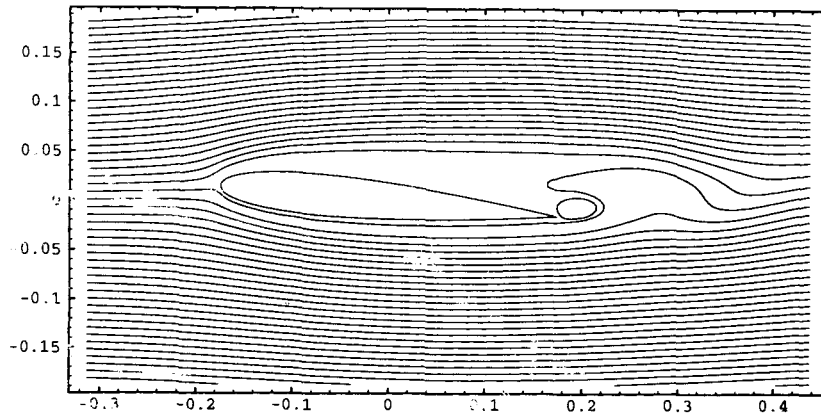


Figure 6. Local enlargement from Plate 2 of the streamlines distribution around NACA0012 with 5 degrees angle of attack

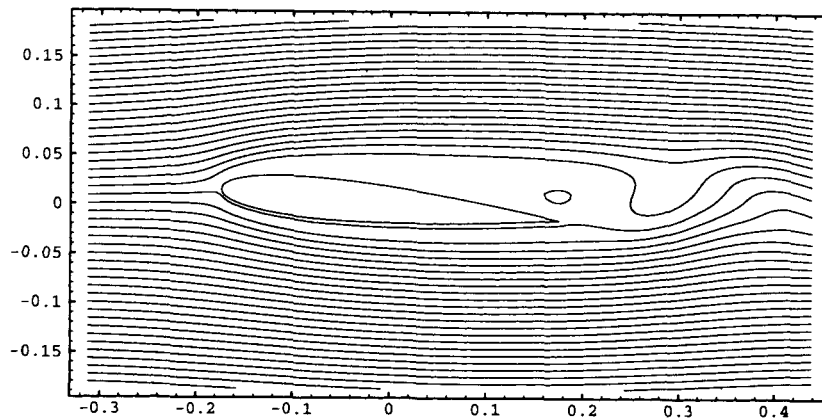


Figure 7. Local enlargement from Plate 3 of the streamlines distribution around NACA0012 with 5 degrees angle of attack

16). Recently, people have tried to apply the fictitious domain approach to these problems (see for example Reference 17). In this section we discuss a fictitious domain approach to a shape optimization problem for Stokes and Navier–Stokes equations in two space dimensions. The shape of a symmetric aerofoil is given by its boundary  $\gamma$ . We fix the chord length of the aerofoil and then parameterize the shape of the wing by 5 parameters, say  $\kappa_i$ , where  $i = 1, \dots, 5$ . By indulging in a slight abuse of notation we can write the boundary,  $\gamma$ , as a function of these 5 parameters. These parameters define the upper (and lower by symmetry) part of the aerofoil by

$$\gamma(\kappa) = \{(x_1, x_2) \mid x_2(x_1) = 5\rho(\kappa_1 x_1^{1/2} + \kappa_2 x_1 + \kappa_3 x_1^2 + \kappa_4 x_1^3 + \kappa_5 x_1^4)\} \quad (65)$$

where  $x_1, x_2$  are the co-ordinates of the upper portion of the boundary of the aerofoil lying above the portion of the wing marked by the  $c$  in the figure below (see Figure 8). Here  $\rho$  is a thickness parameter (for the NACA0012 we take  $\rho = 0.12$ ). The aerofoil is extended to be of length  $c'$  (see Figure 8) by a closed trailing edge (see Reference 18 for further details).

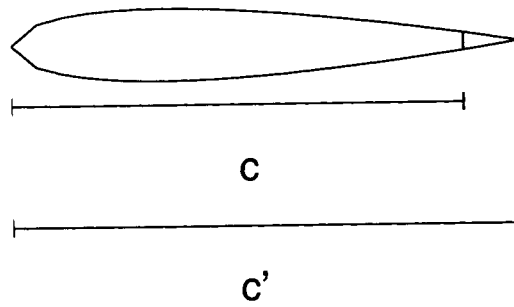


Figure 8

The NACA0012 is described by the parameter values,

$$\kappa^* = (0.2969, -0.126, -0.3516, 0.2843, -0.1015) \quad (66)$$

For every set of parameter values  $\kappa$ , we can employ the ideas and methodology from the preceding sections of this paper to simulate Stokes and Navier–Stokes flow over the aerofoil whose shape is described by a given set of parameters,  $\kappa$ . This simulation yields a velocity field and a pressure distribution. Let  $p^*$  denote the pressure distribution associated with the NACA0012 values for  $\kappa^*$  in (66), hence  $p^*$  is our *target*. Let  $p(\kappa)$  represent the pressure distribution associated with an arbitrary set of parameters  $\kappa$ . We formulate the inverse problem of choosing  $\kappa$  to fit  $p^*$  in the least-squares sense, subject to certain physical constraints. This problem can be formulated as a non-linear programming problem (NLP), namely

$$\min_{\kappa} \|p - p^*\|_{L^2(\gamma)} \quad \text{subject to } K(\kappa) \leq 0 \quad (67)$$

The constraint  $K(\kappa)$  in (67) implements the following constraints:

Any aerofoil whose upper and lower surface intersect in more than two places (the two endpoints of the aerofoil) is infeasible. This can be guaranteed by requiring that  $(\varepsilon_w - x_2|_{\gamma}) \leq 0$  for any  $x_2$  not an endpoint of the aerofoil. Here  $\varepsilon_w$  is a positive minimum aerofoil thickness parameter (for instance, we take  $\varepsilon_w = 10^{-6}$ ). Also included in the constraint function,  $K$ , are obvious physical upper and lower bounds on the volume of the aerofoil,  $\omega$ , the arclength,  $\gamma$ , and the slopes  $\partial\gamma/\partial x_1$  and  $\partial\gamma/\partial x_2$  away from the two endpoints of the aerofoil (see Reference 15 for an overview of problems of this type).

In practice, these constraints save computational work by keeping the minimization procedure away from obviously impossible aerofoil shapes that yield very small objective function values. It is worth noting that for this particular test problem there are no binding constraints at the solution (i.e.  $K(\kappa^*) < 0$ ).

#### 4.1. Optimization technique

While it may be possible to calculate derivatives of the objective function in (67) such a calculation would be extremely expensive and possibly inaccurate. An additional difficulty with using derivatives in the solution of (67) are its many local minimizers and inflection points. Finally, we would enjoy the luxury of using algorithm that allowed us to replace the smooth least-squares objective function in (67) with a continuous but non-differentiable one (for instance an  $L^\infty$  objective function).

Algorithms for unconstrained minimization that require no derivative information (usually referred to as *direct search* or *pattern search* methods) are not new (see, for example, Reference 19 and the references therein). In Reference 20 an algorithm for unconstrained optimization that requires no derivative information was suggested. A parallel implementation of the algorithm has also been developed and tested (see Reference 21). Recently, this algorithm and its implementation have been modified to handle constraints (see Reference 22). The method samples points on the nodes of an evolving pattern, moving to the node in the pattern with the value closest to optimality. Depending on where in the pattern the point closest to optimality was located the pattern then changes, either expanding or contracting. When the pattern expands its overall size grows causing the algorithm to sample points farther from its current location. When the pattern contracts the overall size of the pattern becomes smaller; this procedure terminates when the lengths of the edges of the pattern fall below a user prescribed tolerance.

Pattern search methods of this sort typically do not demonstrate rapid local convergence, but they are extremely robust and far less susceptible than faster higher-order methods to the difficulties introduced when functions are non-smooth or the data are noisy. Pattern search methods are usually too slow to solve optimization problems with large numbers of parameters. Our problem (67) is interesting in that one can accurately describe the shape of an aerofoil accurately with a relatively small number of parameters. The compatibility pattern search method with our problem (67) is also interesting. After numerous numerical tests, we have not failed to locate the global minimum of (67).

#### 4.2. Numerical example

Our numerical example for shape optimization requires integrating equations of the form (17 and 18) to evaluate the objective function. Here, we only consider a zero degree angle of attack for these test problems. For simplicity we keep the same boundary conditions defined by (20) and (21). Parameter values are provided in the tables below (see Tables I and II), except for the parameter  $c$  appearing in (63). We took  $c = 20$  for all our numerical experiments. The cost function column displays, in fact,

$$\|p_c - p^*\|_{L^2(\gamma)} / \|p^*\|_{L^2(\gamma)}$$

where  $p_c$  is the computed pressure.

The minimization was performed in parallel on the Touchstone Delta machine using 16 processors. A coarse/fine strategy was employed to solve the shape of optimization minimization; 10 points per processor were sampled with a very large search strategy to initially a neighbourhood of the solution and then 25 points per processor were sampled with a smaller pattern search

Table I. Coarse minimization: 10 points per processor

$h_p$	$h_v$	$\Delta t$	Reynolds	Function evaluations	Cost function
1/64	1/128	$2.5 \times 10^{-3}$	1000	$2.5 \times 10^2$	$4.9 \times 10^{-1}$
1/64	1/128	$2.5 \times 10^{-3}$	500	$2.5 \times 10^2$	$1.1 \times 10^{-1}$
1/32	1/64	$5.0 \times 10^{-3}$	1000	$1.8 \times 10^2$	$5.7 \times 10^{-1}$
1/32	1/64	$5.0 \times 10^{-3}$	500	$1.8 \times 10^2$	$1.3 \times 10^{-1}$



Table II. Fine minimization: 25 points per processor

$h_p$	$h_v$	$\Delta t$	Reynolds	Function evaluations	Cost function
1/64	1/128	$2.5 \times 10^{-3}$	1000	$2.1 \times 10^2$	$1.8 \times 10^{-4}$
1/64	1/128	$2.5 \times 10^{-3}$	500	$2.1 \times 10^2$	$2.4 \times 10^{-4}$
1/32	1/64	$5.0 \times 10^{-3}$	1000	$1.5 \times 10^2$	$5.7 \times 10^{-4}$
1/32	1/64	$5.0 \times 10^{-3}$	500	$1.5 \times 10^2$	$1.3 \times 10^{-4}$

strategy to polish the solution. For more details on constrained pattern search methods see Reference 22.

## 5. CONCLUSION

Compared to the previous results in Reference 23 it is clear that the fictitious domain methodology that we advocate has been substantially progressing. However, there is still room for improvement particularly concerning the speed-up of the various iterative methods used for the solution of the subproblems obtained from the time splitting. Parallelization is also an important issue currently addressed (see Reference 13).

It appears that the fictitious domain method provides an effective way of evaluating the objective function for the Stokes and Navier–Stokes flow shape optimization problem. In particular, the computational cost of regriding a mesh for every trial airfoil shape could be a prohibitive cost. Current work includes extending these ideas to more complicated objective functions and to the shape optimization problems associated with drag reduction.

## ACKNOWLEDGEMENTS

We would like to acknowledge the helpful comments and suggestions of the following individuals: H. Brezis, L. C. Cowsar, J. E. Dennis, G. H. Golub, R. Hardt, Y. Kuznetsov, W. Lawton, P. Le Tallec, O. Pironneau, J. Pasciak, H. Resnikoff, R. A. Tapia, J. Weiss, R. O. Wells, M. F. Wheeler, O. B. Widlund, V. Torczon, and X. Zhou.

The support of the following corporations and institutions is also acknowledged: AWARE, CERFACS, CRPC, Dassault Aviation, INRIA, University of Houston, Université P. et M. Curie, Rice University. We also benefited from the support of DARPA (Contracts AFOSR F49620-89-C-0125 and AFOSR-90-0334), DRET (Grant 89424), NSF (Grants INT 8612680, DMS 8822522 and DMS 9112847) and the Texas Board of Higher Education (Grants 003652156ARP and 003652146ATP).

Use of the Touchstone Delta Machine located at Caltech was provided by the Center for Research on Parallel Computation funded by the NSF through Cooperative Grant No. CCR-9120008.

## REFERENCES

1. D. P. Young, R. G. Melvin, M. B. Bieterman, F. T. Johnson, S. S. Samanth and J. E. Bussioletti, 'A locally refined finite rectangular grid finite element method. Application to Computational Physics', *J. Comp. Phys.*, **92**, 1–66 (1991).
2. J. E. Bussioletti, F. T. Johnson, S. S. Samanth, D. P. Young and R. H. Burkhart, 'EM-TRANAIR: Steps toward solution of general 3D Maxwell's equations', in *Computer Methods in Applied Sciences and Engineering*, R. Glowinski (ed.), Nova Science, Commack, NY, 1991, pp. 49–72.

3. B. L. Buzbee, F. W. Dorr, J. A. George and G. H. Golub, 'The direct solution of the discrete Poisson equation on irregular regions', *SIAM J. Numer. Anal.*, **8**, 722–736 (1971).
4. R. Glowinski, T. W. Pan and J. Periaux, 'A fictitious domain method for Dirichlet problem and applications', *Comput. Methods Appl. Mech. Eng.*, **111**, 283–303 (1994).
5. R. Glowinski, T. W. Pan and J. Periaux, 'A fictitious domain method for external incompressible viscous flow modeled by Navier–Stokes equations', *Comput. Methods Appl. Mech. Eng.*, **112**, 133–148 (1994).
6. R. Glowinski, T. W. Pan and J. Periaux, 'A Lagrange multiplier/fictitious domain method for the Dirichlet problem. Generalization to some flow problems', *Japan J. Ind. Appl. Math.*, to appear.
7. C. Borgers, 'Domain embedding methods for the Stokes equations', *Numer. Math.*, **57**, 435–451 (1990).
8. R. Glowinski, *Numerical Methods for Nonlinear Variational Problems*, Springer, New York, 1984.
9. M. O. Bristeau, R. Glowinski, B. Mantel, J. Periaux and P. Perrier, 'Numerical methods for incompressible and compressible Navier–Stokes problems', in R. H. Gallagher, G. Garey, J. T. Oden, and O. C. Zienkiewicz (eds.), *Finite Elements in Fluids*, Vol. 6, Wiley, Chichester, 1985, pp. 1–40.
10. R. Glowinski, 'Viscous flow simulation by finite element methods and related numerical techniques', in E. M. Murman and S. S. Abarbanel (eds.), *Progress and Supercomputing in Computational Fluid Dynamics*, Birkhauser, Boston, 1985, pp. 173–210.
11. M. O. Bristeau, R. Glowinski and J. Periaux, 'Numerical methods for the Navier–Stokes equations', *Comp. Phys. Rep.*, **6**, 73–187 (1987).
12. R. Glowinski, 'Finite element methods for the numerical simulation of incompressible viscous flow. Introduction to the control of the Navier–Stokes equations', *Lectures in Applied Mathematics*, **28**, AMS, Providence, R. I., 1991, pp. 219–301.
13. R. Glowinski, T. W. Pan and J. Periaux, 'A one shot domain decomposition/fictitious domain method for the solution of elliptic equations', to appear.
14. O. Pironneau, *Finite Element Methods for Fluids*, Wiley, Chichester, 1989.
15. O. Pironneau, *Shape Optimization*, Springer, New York, 1984.
16. D. Begis and R. Glowinski, 'Application de la méthode des éléments finis à l'approximation d'un problème de domaine optimal. Méthodes de résolution des problèmes approchés', *Appl. Math. Optim.*, **2**, 130–169 (1975).
17. J. Haslinger, 'Embedding/control approach for solving optimal shape-design problems', *East-West J. Numer. Math.*, **1**(2), 111–119 (1992).
18. A. J. Kearsley, 'Optimization methods for partial differential equations from science and engineering', *Ph.D. Dissertation*, Department of Computational and Applied Mathematics, Rice University, Houston, TX, 1995.
19. J. Céa, *Optimisation: Théorie et Algorithmes*, Dunod, Paris, 1971.
20. J. E. Dennis, V. Torczon, 'Direct search methods on parallel machines', *SIAM J. Optim.*, **1**, 448–474 (1991).
21. V. Torczon, 'PDS: direct search methods for unconstrained optimization on either sequential or parallel machines', *TOMS, Trans. Math. Software*, to appear.
22. A. J. Kearsley, R. A. Tapia and V. Torczon, 'On the use of parallel direct search methods for nonlinear programming problems', *Technical Report #93-33*, Department of Computational & Applied Mathematics, Rice University, Houston, TX, 1993.
23. R. Glowinski, T. W. Pan J. Periaux and M. Ravachol, 'A fictitious domain method for the incompressible Navier–Stokes equations', in E. Oñate, J. Periaux, A. Samuelson (eds.), *The Finite Element Method in the 90's*, Springer, Berlin, 1991, pp. 440–417.